Self-Sustained Oscillation of a Turbulent Jet Flow in Hot Cavity

Iachachene Farida[#1], Mataoui Amina[*2]

[#] *Department of physic, faculty of sciences*

University M'hamed Bouguerra Boumerdes UMBB, Boumerdes, Algeria

**Theoretical and applied laboratory of fluid mechanics,*

University of sciences and Technology Houari Boumedienne- USTHB.

[1]iachachenef@yahoo.fr

Abstract— **Computations of heat transfer and fluid flow of an isothermal two-dimensional jet flowing into a rectangular hot cavity are reported in this paper. Both velocity and temperature distributions are predicted by solving the two-dimensional Unsteady Reynolds Averaged Navier–Stokes (URANS) equations. This approach is based on one point statistical turbulence modeling using the energy - specific dissipation (k-ω) model. The numerical predictions are achieved by finite volume method. This problem is relevant to a wide range of practical applications including forced convection and the ventilation of mines, enclosure or corridors. The structural properties of the flow and heat transfer are described for several conditions. An oscillatory regime is evidenced for given jet location, inducing a periodic behavior versus time. The jet flapping phenomena is detailed numerically by the instantaneous streamlines contours and the isotherms within one period of oscillation. The heat transfer along the cavity walls is also periodic. Time average of mean Nusselt number is correlated according with some problem parameters**

Keywords— **Impinging jet; Nusselt number; self-oscillation; turbulence; cavity**

I. INTRODUCTION

Since more than half of century ago, heat transfer by impinging jet was subject to a great interest in several industrial and engineering applications, because the high heat and mass transfer coefficients can be obtained around a jet stagnation region and the heat transfer characteristics can be easily controlled. Many publications have confirmed the dependence of the heat transfer with some number of parameters, such as Reynolds number, temperature, the impinging distance, the lateral confining wall and the nozzle shape [1,7]. The present work is on the subject of a plane isothermal fully developed turbulent jet issuing into a rectangular hot cavity (fig1). Many researchers [8-13] shown that, when the jet is set in the mid-plane of a cavity, an oscillatory flow occurs. These self-sustained oscillations are generated by an instability produced by the configuration of a plane jet located between two symmetrical lateral vortices .For non-symmetrical case of the jet location in the cavity, the same phenomenon occurs and sometimes is reinforced [12]. But, when the jet width is reduced compared at that of cavity, from a certain width, these oscillations are attenuated because the third component of the velocity in the z-direction becomes significant due to the side wall effect and a 3D flow is occurred. For this reason, the case of a circular jet in a cylindrical cavity is always steady in average (Halouane et al. [7], Zidouni et al. [5]). So one may consider this problem bidimensional.

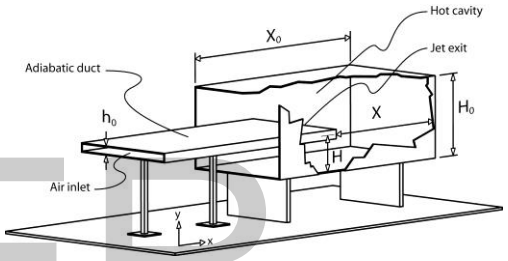

Fig 1. Configuration, jet hot cavity interaction

II. PROBLEM STATEMENT

The fluid is assumed in average Newtonian and incompressible with constant thermo physical properties. The URANS equations for incompressible flow in Cartesian coordinates are deduced from the mass, momentum and energy balance equations, coupled with the equations of the turbulent quantities as follows:

Mass conservation equation: $$\frac{\partial U_i}{\partial x_i} = 0 \qquad (1)$$

Momentum conservation equation:

$$\rho\frac{\partial U_i}{\partial t}+\rho U_j\frac{\partial U_i}{\partial x_j}=-\frac{\partial P}{\partial x_i}+\frac{\partial}{\partial x_j}\left(\mu\frac{\partial U_i}{\partial x_j}-\rho\overline{u_i u_j}\right) \qquad (2)$$

Energy conservation equation:

$$\rho\frac{\partial T}{\partial t}+\rho U_i\frac{\partial T}{\partial x_i}=\frac{\partial}{\partial x_i}\left(\frac{\mu}{pr}\frac{\partial T}{\partial x_i}-\rho\overline{u_i\theta}\right) \qquad (3)$$

Where P, T and U_i are mean pressure, temperature and velocity components respectively. θ and u_i are the temperature fluctuation and velocity components fluctuations, respectively. x_i is the space coordinates and t is the time. The fluid properties ρ, μ and Pr are respectively density, dynamic viscosity and Prandtl number. In this paper, the closure of the equations is achieved using the SST energy- specific dissipation rate (k-ω) turbulence model (Menter [14] ,Wilcox[15]).

Fig2 reports the dynamical, thermal and geometrical conditions of the present study. Constant values of inlet boundary conditions are imposed as follow:

$U=U_0$, $V=0$, $k_0=0.03U_0^2$, $\varepsilon_0=\frac{k_0^{3/2}}{\lambda h_0}(\lambda=0.1)$, $\omega_0=\frac{1}{c_\mu}\frac{\varepsilon_0}{k_0}$, $T=T_0$

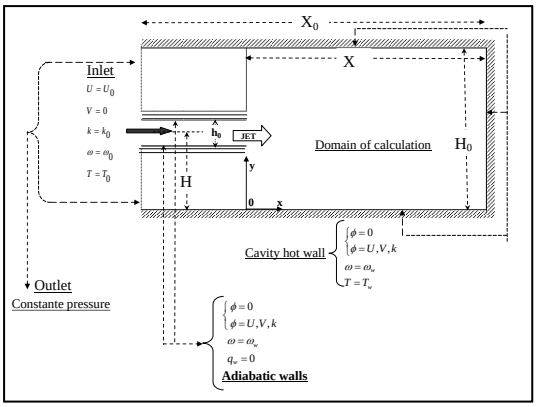

Fig 2. Boundary conditions and parameters

The solution domain was meshed by divided it quadrilateral cells. The non-uniform structured grids were used. Refinements before and after the nozzle exit were managed in order to describe the entrainment accurately. Sufficiently fine grids were used near the cavity and duct walls to predict very high gradient of variables prevailed in the viscous sub-layer (fi g3).

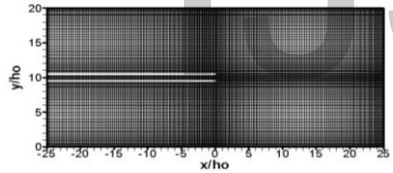

Fige 3. Typical grid of the jet–cavity interaction

ANSYS FLUENT 14.0 CFD[16] code is used as a tool for numerical solution of the governing equations based on finite-volume method (Patankar, S.V. 1980[17]). POWER LAW discretization scheme is selected for convection-diffusion formulation for momentum and energy equations and second order scheme for the pressure. The discretized equations were solved following the SIMPLE algorithm. For time integral the first order implicit scheme is used, which is unconditional stable.

III Results and Discussion

For each case, a grid independency test is carried out by refining and adjusting the grid in the two directions. Fig 4 shows the effect of grid size on the average Nusselt number distribution on the cavity bottom and laterals walls for the jet-cavity interaction, $L_f = 25$ and $L_h = 10$. It is observed that grid independence is achieved at 220 × 120 distributions beyond which no further significant change in average Nusselt number distribution is noticed, we have chosen this grid to save computational time. The grid independence tests are checked for each jet-cavity interaction. Additionally, the influence of the time step is also deepened. Knowing that the frequencies of oscillation of jet flapping are relatively low, a first order time scheme is achieved for time interpolation. For each case, the courant number is about unity for the most part of the flow field.

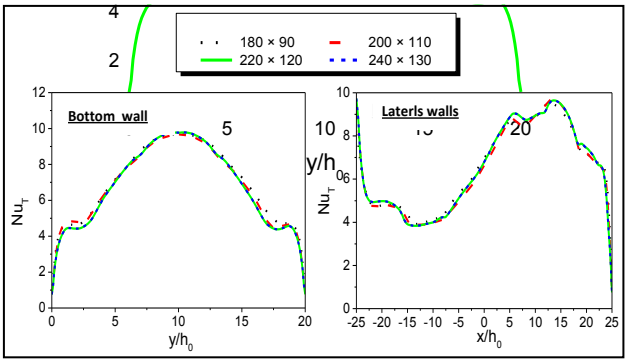

Fig 4. Effect of grid refinement for (L_f =25and L_h=10) and Re =4000

For a given jet location inside the cavity ($L_h = 8.5$, $L_f = 30$), fig5. shows the Fourier transforms of the velocity components time signals, the mean pressure and the mean temperature at several points. The first peak of the Fourier modes distribution accurately determines the fundamental frequency. This figure confirms the periodic behavior of dimensionless time-averaged of each variable, for a given Reynolds number, the period of the oscillation is analogous at all point of the configuration.

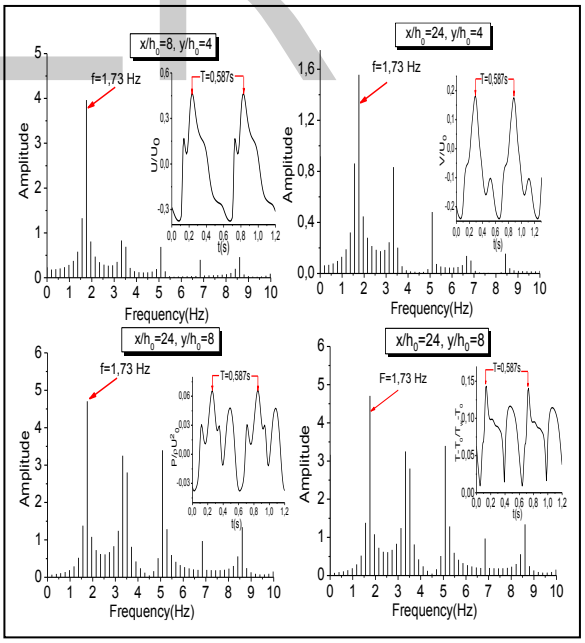

Fig5. Fourier modes

Fig6 shows four stages during one period of oscillation, for a given Reynolds number of Re = 4000 and jet exit location of L_h=8.5, L_f=40; the experimental visualization photo of Mataoui et al. [12] and their corresponding computed values of the vorticity magnitude contours and the streamlines contours . Furthermore, the reverse flow at the opposite side of the impingement of the jet is highlighted at each instant.

IJSER

Qualitatively, good agreement is obtained between the two predictions. The jet in the cavity generates the development of two main counter rotating eddies on each side of the jet. These two eddies are evidenced by the calculated streamlines and vorticity contours. The vortical structures follow the motion of the jet flapping. Instantaneously, vorticity magnitude is significant within the shear layer of the jet, all eddies center and close to the cavity wall. Furthermore, at the cavity corners, one detects some secondary eddies. One also observes, that each two neighboring eddies are counter rotating. The oscillatory phenomenon is due to the instability generated by the pattern of a jet flowing between two eddies. Therefore, the self-sustained oscillations are produced by the periodic deflection of the jet axis due to the Coanda effect (Shakouchi [10], Mataoui et al. [12]and Mataoui and Schiestel [13]).

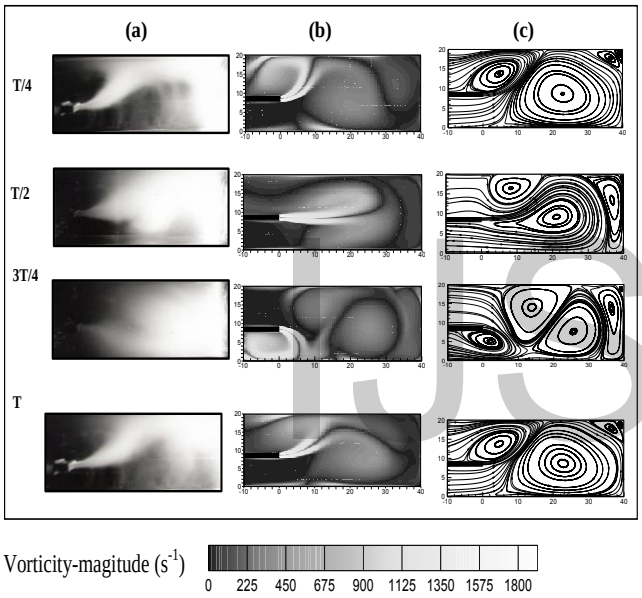

Fig 6. Flow structure :(a) experimental flow visualization (Mataoui et al. [12]).
(b) contours of vorticity magnitude and (c) streamlines contours

For the thermal study, the instantaneous field temperature and the streamlines contours for each 1 / 8th period of oscillation for a Reynolds number Re = 6000 and jet exit location (L_f = 25, L_h = 8.5) are illustrated in fig 7. Due to the oscillatory aspect of the jet, the cooling of the confined space of the cavity varies over time. The exchange of heat is great in the stagnation region which changes its position over time. Development of a thermal boundary layer in the vicinity of each hot wall. An important heat exchange occurs in the region of interaction of two counter rotating vortices. While the two vortices interaction zone which rotates in the same direction does not entail any decrease in the heat. The aspiration phenomena is clearly visible in this figure, a reversal in the aspiration of air between the lower and upper outlet sections of the cavity is carried out over time. This aspiration caused a cooling of the wall which is adjacent of the cavity outlet where aspiration occurs.

The variation of instantaneous local Nusselt number along the three walls of the cavity during one period, for the case L_f = 25 and L_h = 8.5, Re = 6000 are illustrated in fig8. The local Nusselt number varies versus time and position; it is deduced from the temperature gradient at the hot plate as:

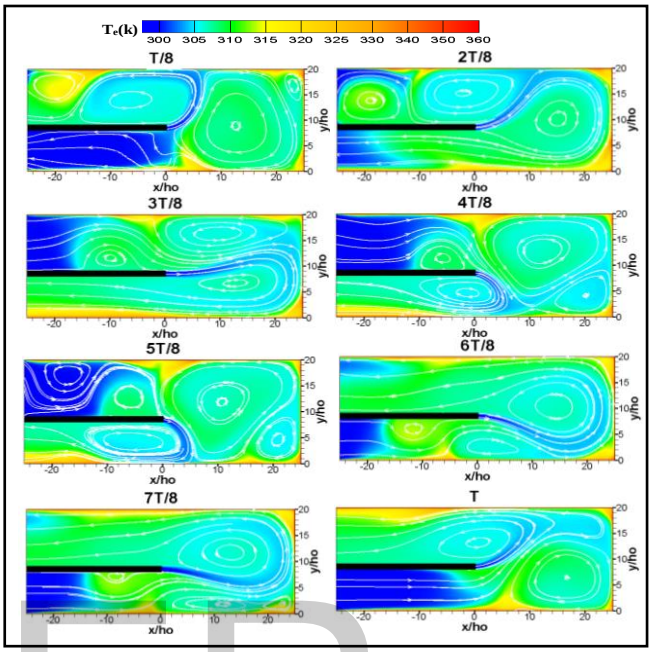

Fig7. The temperature field.

$$Nu(t,x) = -\left(\frac{h_0}{T_H - T_C}\right)\left(\frac{\partial T}{\partial n}\right)_{ywall} \quad (4)$$

Where *n* is the perpendicular direction to the corresponding wall.

In this figure the streamlines contours justify the Nusselt number variation, particularly the stagnation point's location where the jet impinges the wall. The deflection of the jet induces dissimilar local Nusselt number distribution on each cavity wall. Since the heat transfer rate is closely related to the flow pattern behavior. It is observed from this figure that each maximum Nusselt number corresponds to the stagnation points of the jet. We note also several secondary peaks in the distribution of the Nusselt number; these maxima are points of interaction of two counter rotating vortices that develop by moving and changing volume over time.

To examine the effect of jet location and Reynolds number, on the overall flow and heat transfer process, the instantaneous variation of the instantaneous average Nusselt number at each cavity wall is deduced by integrating it over the length of the corresponding wall, as follows:

$$Nu_{avr}(t) = \frac{1}{L}\int_0^L Nu(t,l)dl$$

The instantaneous average Nusselt number varies periodically for all analyzed cases of this study. For the symmetrical interaction (L_h=10), fig 9 shows the variations of the instantaneous average Nusselt number of the upper and lower side cavity walls. Similar trend is obtained for all horizontal impinging distance (L_f). Moreover, instantaneous average Nusselt numbers of the upper and lower walls are fully

IJSER

coupled: a maximum peak of Nu_{avr}(upper wall) corresponds to a minimum value for the Nu_{avr}(lower wall) and vice versa. The two signals are in opposite phases for the side cavity walls. On the other hand, the Nusselt number on the bottom is closely related to the horizontal impinging distance L_f, when L_f decreased Nu_{avr}(bottom wall) increases. However, the shape of the instantaneous signals of Nu_{avr}(bottom wall) is completely different due to the symmetrical flapping motion of the jet (for one period the jet impinges the bottom twice), the frequency of the signal is twice of the frequency of the phenomenon.

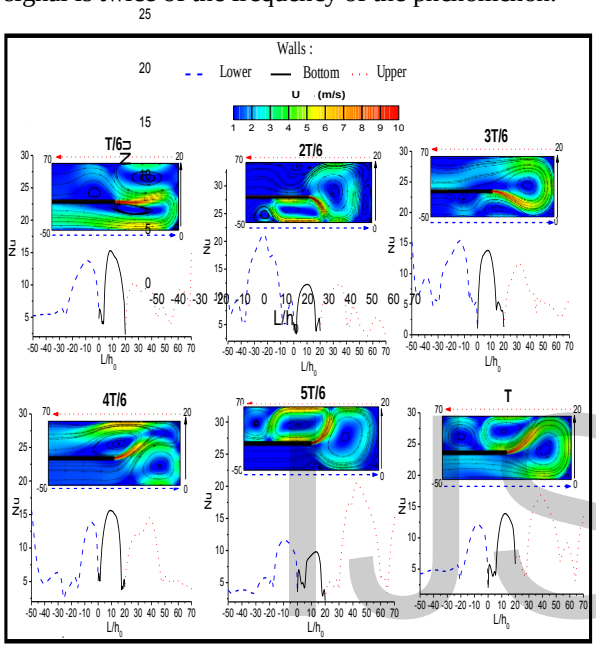

Fig.8 The streamlines and the local Nusselt number for the three walls of the cavity(L_f=25 and L_h=8.5 Re=6000)

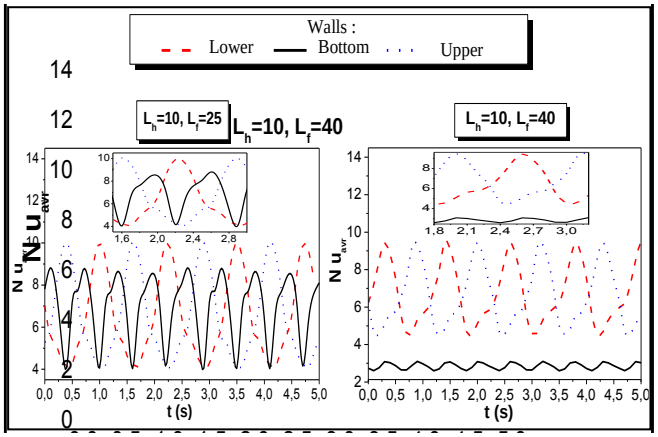

Fig.9 Average Nusselt number of the three walls of the cavity Re=4000

The effect of the Reynolds number on the instantaneous average Nusselt number along of all the walls is given in fig. 10. This figure confirms that the increasing of Reynolds number enhances the heat transfer for the three cavity walls. Furthermore, the frequency of oscillation increases when Reynolds number augments like the flow field. This result reproduces the available experimental data of Mataoui et al. [12].

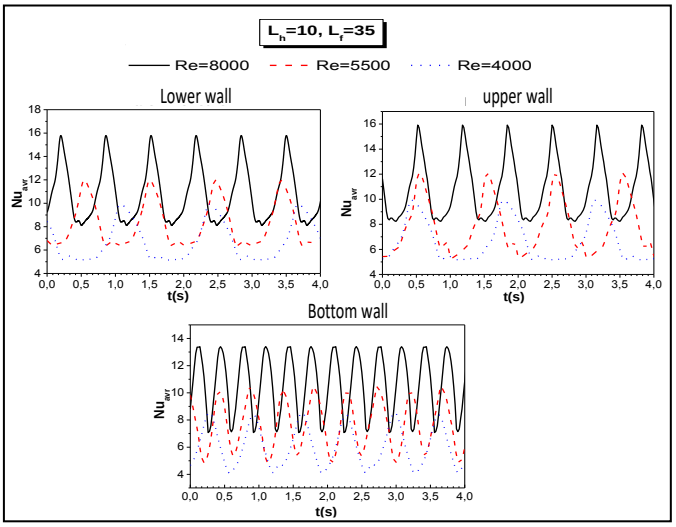

Fig10. Influence Reynolds number on the average Nusselt number for the three walls of the cavity

In fig 11, we have plotted the evolution of average Nusselt number ($\overline{Nu} = \frac{1}{T}\int_0^T Nu_{avr}(t)dt$)on the walls of the cavity according to the impact distance L_f for different values of Reynolds number and for two heights of the jet (symmetrical case L_h = 10 and asymmetrical case L_h = 6.5). The analyses of this figures leads to the following observations:

- The increase of Reynolds number enhances the heat transfer on all the walls of the cavity.
- The evolution in the average Nusselt on the bottom is closely related to the impact distance L_f, increasing of L_f reduces the heat transfer.
- However, on the two laterals walls of the cavity, increasing the impact distance has a slight influence on the heat transfer mainly for the symmetrical case (L_h=10).
- The heat transfer on the side walls of the cavity depends of the height of the jet, for a symmetrical position of the jet the value of the average Nusselt number is the same on both upper and lower side walls. As for the asymmetric case the exchange of heat is less intense on the nearest wall of the jet exit.

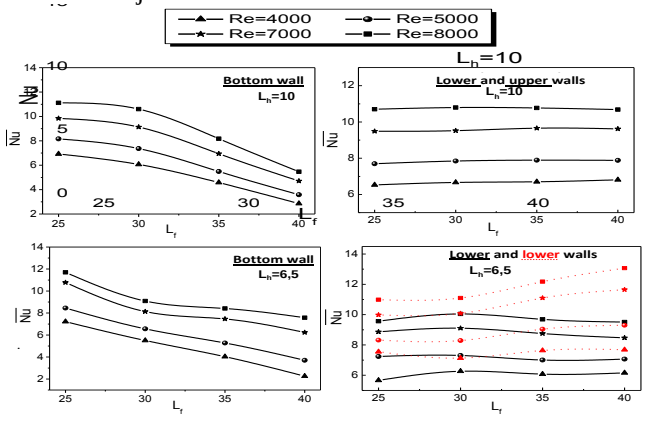

Fig11. Effect of impinging distance on mean Nusselt number for the three walls of the cavity

IJSER

The effect of the position of the jet into the cavity on the average Nusselt number along all walls is illustrate in fig 12.
The figure shows that the heat transfer is closely related to the impinging distance (L_f) and the Reynolds number Re. However, the height of the jet slightly affects.

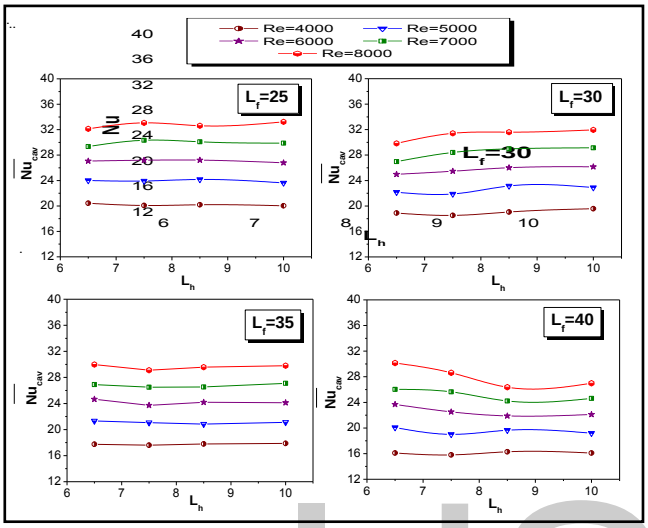

Fig 12. Effect of the position of the jet on mean Nusselt number for the three walls of the cavity

For three heights of the jet The average Nusselt numbers $\overline{Nu}_{cavity}$ are correlated with jet Reynolds number and nozzle–to-bottom wall distance L_f, following the curve fitting technique using least-squares method as shown in fig13. This correlation is obtained with a maximum error of 2% in comparison to the predicted values of average Nusselt number .

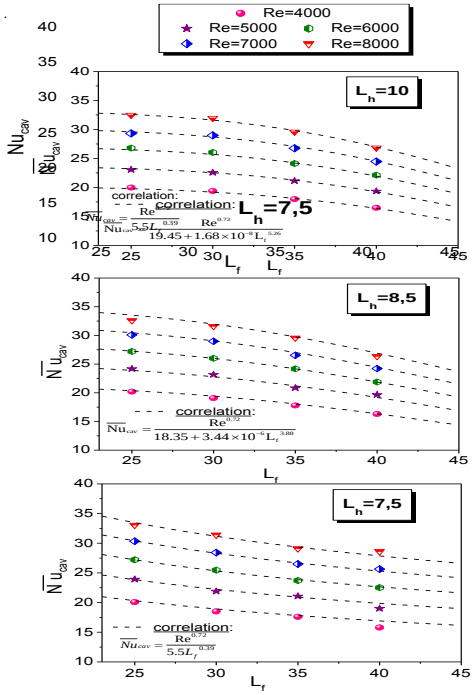

Fig13. Mean Nusselt number distribution with Reynolds number

CONCLUSIONS

A comprehensive numerical simulation for the forced convection heat transfer of a slot jet impinging a hot rectangular cavity is examined in this work using one point closure turbulence model. Depending on the location of the jet exit inside the cavity several flow regimes occur. In this paper, we have focused on the heat transfer self-oscillation phenomenon. The comparison of the flow structure by the present simulation with experimental results shows a good agreement is obtained qualitative and quantitative. For a given jet location inside the cavity, all variables have a periodic behavior versus time with the same frequency. Deflection of the jet is verified numerically by the instantaneous streamline contours within a period of time.
Due to the self-oscillation of the jet, the three walls of the cavity are cooled simultaneously. The heat transfer along the cavity walls is also periodic and depends on the variation of the size of the eddy at each instant. For each cavity wall, the numerical predictions show that the instantaneous average Nusselt is also periodic with the same period than that of the flow field. The time evolution of local Nusselt number for the symmetrical interaction of the side walls of the cavity are in opposite phase (same magnitude). The heat transfer is closely related to the impinging distance (L_f) and the Reynolds number Re. However, the height of the jet slightly affects. The evolution of average Nusselt number is correlated according to the impinging distance and Reynolds number.

REFERENCES

[1] Martin, H., (1977),''Heat and mass transfer between impinging gas jets and solid surfaces", *Advances in Heat Transfer*, 13, Academic Press, New York, pp. 1–60.
[2] Li,P. W. and. Tao, W. Q, (1993),''Numerical and experimental investigations on heat/mass transfer of slot-jet impingement in a rectangular cavity", *Int. J. Heat and Fluid Flow* Vol. 14 (3) ,pp 246-253.
[3] Brignoni L. A., and Garimella S. V., (2000);" Effect of Nozzle Inlet Chamfering on Pressure and Heat Transfer in Confined Air Jet Impingement", *Int. Journal of Heat and Mass Transfer*, vol. 43, pp. 1133-1139.
[4] Chan, T.L., Leung, C.W., Jambunathan, K., Ashforth-Frost,Y. S., Zhou, Liu,M.H., (2002);"Heat transfer characteristics of a slot jet impinging on a semi-circular convex surface", *Int.J. Heat Mass Transfer* ,Vol. 45, pp 993-1006.
[5] Zidouni–Kendil F. , Mataoui A., A. Benaissa A., (2009),"Flow Structures of a Round Jet Evolving Into a Cylindrical Cavity, International Journal of Transport Phenomena", Vol. 11, No. 2, pp. 165-183.
[6] Benmouhoub,D, Mataoui, A., (2013),"Turbulent Heat Transfer From a Slot Jet Impinging on a Flat Plate", Journal of Heat Transfer(ASME), (2013), Vol. 135 pp.
[7] Halouane,Y., Mataoui,A. Iachachene,F., "Heat Transfer Prediction of a Jet Impinging a Cylindrical Deadlock Area", Journal of Heat Transfer(ASME), (2014), Vol. 136 pp
[8] Ogab A., (1985), ''Contribution a L'étude de L'évolution d'un Jet Plan Turbulent dans une Cavité de Section Rectangulaire'', Thèse De Magister, Mécanique Des Fluides, Usthb Alger.
[9] Shakouchi, T., Kuzuhara, S. and Yamaguchi, J., (1986),''Oscillatory Phenomena of an Attached Jet''. *Bull. Jsme* 29 1117–1123.

IJSER

[10] Shakouchi T., (1989),''A New Fluidic Oscillator, Flowmeter, Without Control Port and Feedback Loop'', *J. Dyn. Syst. Measur.Control* 111, 535–539 .
[11] Shakouchi T., Suematsu Y. and Ito T, A study on oscillatory jet in a cavity, Bull. JSME 25 (206) (1982) 1258–1265.
[12] Mataoui A. , Schiestel R. & Salem A. , (2001),''Flow Regimes of Interaction of a Turbulent Plane Jet Into a Rectangular Cavity :Experimental Approach and Numerical Modelling'' ,Journal of Flow, *Turbulence and Combustion* ,Vol . 67 (4): pp. 267-304.
[13] Mataoui, A. and Schiestel, R , (2009);''Unsteady phenomena of an oscillating turbulent jet flow inside a cavity: Effect of aspect ratio'',*Journal of Fluids and Structures*, Vol. 25,pp 60–79.
[14] Menter F. R, (1994),'' Two-Equation Eddy-Viscosity Turbulence Models for Engineering Applications'', *AIAA Journal*, 32(8)1598-1605.
[15] Wilcox D. C**.** (1994);'' Turbulence Modelling for CFD, DCW Industries Inc''; La Canada, CA,
[16] ANSYS FLUENT 14.0 CFD code Documentation.
[17] Patankar, S.V. (1980),"Numerical heat transfer and fluid flow", Series in computational methods in mechanics and thermal sciences, hemisphere Publiching Corporation.
[18] S. M. Metev and V. P. Veiko, *Laser Assisted Microtechnology*, 2nd ed., R. M. Osgood, Jr., Ed. Berlin, Germany: Springer-Verlag, 1998.
[19] J. Breckling, Ed., *The Analysis of Directional Time Series: Applications to Wind Speed and Direction*, ser. Lecture Notes in Statistics. Berlin, Germany: Springer, 1989, vol. 61.
[20] S. Zhang, C. Zhu, J. K. O. Sin, and P. K. T. Mok, "A novel ultrathin elevated channel low-temperature poly-Si TFT," *IEEE Electron Device Lett.*, vol. 20, pp. 569–571, Nov. 1999.
[21] M. Wegmuller, J. P. von der Weid, P. Oberson, and N. Gisin, "High resolution fiber distributed measurements with coherent OFDR," in *Proc. ECOC'00*, 2000, paper 11.3.4, p. 109.
[22] R. E. Sorace, V. S. Reinhardt, and S. A. Vaughn, "High-speed digital-to-RF converter," U.S. Patent 5 668 842, Sept. 16, 1997.
[23] (2002) The IEEE website. [Online]. Available: http://www.ieee.org/
[24] M. Shell. (2002) IEEEtran homepage on CTAN. [Online]. Available: http://www.ctan.org/tex-archive/macros/latex/contrib/supported/IEEEtran/
[25] *FLEXChip Signal Processor (MC68175/D)*, Motorola, 1996.
[26] "PDCA12-70 data sheet," Opto Speed SA, Mezzovico, Switzerland.
[27] A. Karnik, "Performance of TCP congestion control with rate feedback: TCP/ABR and rate adaptive TCP/IP," M. Eng. thesis, Indian Institute of Science, Bangalore, India, Jan. 1999.
[28] J. Padhye, V. Firoiu, and D. Towsley, "A stochastic model of TCP Reno congestion avoidance and control," Univ. of Massachusetts, Amherst, MA, CMPSCI Tech. Rep. 99-02, 1999.
Wireless LAN Medium Access Control (MAC) and Physical Layer (PHY) Specification, IEEE Std. 802.11, 1997.

IJSER